Sessile Liquid Marbles with Embedded Hydrogels as Bioreactors for Three-Dimensional Cell Culture

Raja Vadivelu, Navid Kashaninejad,* Mohammad Reza Nikmaneshi, Rubina Rahaman Khadim, Seyedeh Sarah Salehi, Naveen Chintala Ramulu, Yasuyuki Sakai, Masaki Nishikawa, Bahar Firoozabadi, and Nam-Trung Nguyen*

Digital microfluidics based on liquid marble (LM) has recently emerged as a promising platform for liquid handling and cell-based assays. However, evaporation is a critical problem in such platforms, hindering their wide-range applications in various fields. This study aims to develop a functional sessile LM system for long-term 3D cell culture. Previously, this study group and others demonstrated that floating LM-based bioreactors could reduce the evaporation rate, and were thus suitable for growing multicellular spheroids. However, floating LMs are not robust and easily collapse. Herein, an evaporation-reducing sessile LM by embedding LM with agarose gel is proposed. Through a series of comprehensive mathematical modeling, numerical simulations, and experimental investigations (both with and without biological cells), it is shown that such a platform acts as a moisture absorption system to control the evaporation and thus extends the life span of LMs. It is also found that unlike pure LMs, the LMs filled with agarose maintain their spherical shapes within 72 h inside a humidified incubator. Moreover, the presence of agarose significantly contributes to minimizing evaporation and improves the viability of the harvested multicellular spheroids. These results can open up a new avenue in using LMs in life sciences and chemistry.

1. Introduction

A liquid marble (LM) is formed by coating the surface of a droplet with microparticles,[1] usually by rolling it on a bed of hydrophobic particles.[2] The hydrophobic coating creates an elastic and robust hydrophobic shell with nonadhesive properties. Moreover, an LM simplifies liquid handling and manipulation benefiting the chemical and biological applications, including 1) serving as a microbioreactor with a small volume; 2) mixing a small volume by coalescence; and 3) splitting. Due to the small size of microparticles, LMs possess a large apparent contact angle on any solid surface.[3] The large apparent contact angle, on the order of 150°, allows LMs to move rapidly on a surface without any leakage.[4] Interestingly, the coating of microparticles in LMs acts as a porous barrier, thus allowing the exchange of gases.[5,6] It was also demonstrated that the properties of LMs depend on the hydrophobicity of the microparticles.[7] More importantly, these layers of microparticles can also decrease the evaporation rate[8] and significantly extend the lifetime of LM compared to that of pure droplets. The lifetime depends on the particle coating that serves as a protective layer against evaporation and maintains its spherical shape. The lifetime also depends on the surface/volume ratio. Smaller LMs, i.e., 10 µL, are more robust but may suffer from the higher evaporation rate.

Several studies in the literature compared the evaporation rate and the lifetime of LMs with those of pure droplets. For instance, Dandan et al. reported that the lifetime of a pure water droplet was almost half of that of an LM coated with graphite powder.[9] Doganci et al. reported that the coating of graphite microparticles delays the evaporation of the aqueous phase within LMs, thus retaining the spherical shape of the LM for an extended time.[10]

Dr. R. Vadivelu, Dr. N. Kashaninejad, Prof. N.-T. Nguyen
Queensland Micro- and Nanotechnology Centre
Nathan Campus
Griffith University
170 Kessels Road, Brisbane, QLD 4111, Australia
E-mail: n.kashaninejad@griffith.edu.au; nam-trung.nguyen@griffith.edu.au

Dr. R. Vadivelu, R. R. Khadim, Prof. Y. Sakai, Prof. M. Nishikawa
Department of Chemical System Engineering
School of Engineering
The University of Tokyo
Tokyo 113-8656, Japan

M. R. Nikmaneshi
Cancer Center
Massachusetts General Hospital
Harvard Medical School
Boston, MA 02115, USA

M. R. Nikmaneshi, S. S. Salehi, Prof. B. Firoozabadi
Department of Mechanical Engineering
Sharif University of Technology
Tehran 11365–11155, Iran

N. C. Ramulu
Griffith Sciences
Nathan Campus
Griffith University
170 Kessels Road, Brisbane, QLD 4111, Australia

ADVANCED
SCIENCE NEWS
www.advancedsciencenews.com

ADVANCED
BIOLOGY
www.advanced-bio.com

In parallel, 3D microfluidic cell culture systems have attracted heaps of attention in highly multidisciplinary fields such as tissue engineering, regenerative medicine, cancer research, stem cell biology, and drug discovery.[11] These fields require the generation of 3D tissue constructs at the higher physiological integrity and viability.[12] For instance, the formation of viable spheroids necessitates a condition of cell culture subject to lower evaporation rate. In a previous study, we showed that the evaporation rate was crucial for the development of multiple spheroids oft the same size.[13] Additionally, long-term culture using LM is critical creating microenvironment for studying cell–cell interaction,[14,15] enhancing the maintenance of stem cell pluripotency,[16] and organoid culture.[17]

However, one of the drawbacks of cell culture using LM is fluid loss due to excessive evaporation.[13] This issue of evaporation is more pronounced in LM-based cell culture platforms and determines how long an LM-based bioreactor can last. One possible solution to extend the lifetime of an LM is the use of low molecular weight microparticles to float the LM on top of a liquid, instead of a solid surface. For instance, Gao and McCarthy showed that ionic LMs prepared by coating the water droplets with oligomeric tetrafluoroethylene (OTFE) particles remained floating on water for several weeks.[18] In our previous study, we demonstrated that floating LM (FLMs) could also be used for cell culture application.[13] We showed that FLMs slowed down the evaporation rate and was useful for growing cell spheroid. In a floating system, the coating layer of LM and surface of the liquid bath is detached with a thin air pocket layer, this interface facilitates absorption of water molecules into the LM and subsequently reduce the loss of mass due to evaporation process. However, FLMs possess certain limitations in terms of stability and dispensability. Notably, FLMs are fragile and can be easily broken. These limitations hinder the application of FLMs for long-term cell culture. In this regard, a sessile LM will be more reliable in the aspects of liquid handling.

Recently, we introduced a unique sessile LM system with an embedded hydrogel sphere, which can act as a bioreactor for growing 3D doughnut-like, toroidal tissues,[19] and improve cell cryopreservation.[20] Moreover, liquid-overlay method on agarose was shown to reduce evaporation[21] and improves multiple spheroid growth. Therefore, it is interesting to reduce the evaporation rate of LM with an embedded agarose hydrogel sphere. Also, lowering the evaporation rate in LM prevents its the spherical shape from becoming inflated, especially for cell culture applications, where the integrity of an LM needs to be maintained for an extended cell culture duration.[22] To overcome these issues, we adopt agarose-embedded LM to function as an evaporation-reducing microbioreactor. To address the advantage of agarose gel in reducing evaporation, the mass change of the agarose-embedded LM was measured over time. Based on the experimental data and mathematical modeling, we derive an empirical equation to determine the evaporation rate of both LM and LM with an embedded hydrogel of different agarose concentrations. Next, we experimentally evaluate the effect of relative humidity (RH) on the collapse time of LMs with and without hydrogel. Following that, the lifetime of agarose-embedded LM containing biological cells was systematically investigated, and the results are compared to those of pure LMs. Additionally, in this study, as a proof of concept, we load agarose containing fetal

bovine serum (FBS) inside the LM to serve as a slow-release carrier. The release FBS from the agarose gel into the surrounding cell suspension yields multiple spheroid growth. This concept has the advantage of increasing the potency of growth factors and maintaining their bioactivity for an extended period.

2. Experimental Section

2.1. Preparation of Low-Melting-Point Hydrogel

Using low-melting-point agarose powder (Invitrogen #16520050), three different concentrations of agarose hydrogel were prepared. To this aim, 0.025, 0.05, and 0.1 g of agarose powder were dissolved in a fixed volume of deionized (DI) water (i.e., 10 mL). Accordingly, these three different agarose solutions with weight/volume percentages of 0.25%, 0.5%, and 1% were heated up on a hot plate at 90 °C and stirred for ≈1–2 min to facilitate complete dissolution. Finally, each solution was placed in a water bath at 40 °C to prevent solidification.

2.2. Preparation of LMs with Embedded Agarose Hydrogels

In this study, three different LMs were produced with embedded agarose hydrogel by using three different liquids, i.e., DI water, cell culture medium (DMEM/F-12; Gibco #11320033), and cell culture medium containing biological cells (i.e., human mammary fibroblast (HMF)). All the cells were obtained from the American Type Culture Collection. The schematic representation of the formation process of these LMs is depicted in **Figure 1**. Polytetrafluoroethylene (PTFE) powder was used with a nominal particle size of 1 μm (Sigma-Aldrich #430935). The powder was deposited and distributed into a six-well plate to create an evenly layered powder bed. First, 5 μL of agarose solution that was kept in a water bath (as described in the previous section) was immediately placed on the well containing the PTFE powder (Figure 1A) and incubated for 2 min at room temperature for solidification (Figure 1B). Then, 10 μL of DI water, or DMEM/F-12 without cells, or DMEM/F-12 with HMF cells was dispensed vertically on top of a sessile agarose gel on a PTFE to generate a compound droplet (Figure 1C,D). The marbles were subsequently picked by sucking up using 1000 μL pipette tips that were cut at the edge to accommodate the LM and then dispensed into a flat substrate. Next, the platform was tilted Figure 1E, and the compound droplet was rolled on the powder bed in a circular motion in order to form a robust LM containing water and the agarose gel (Figure 1F). It should be noted that to prepare the pure LM without any agarose gel, 15 μL of DI water was directly deposited in the well containing the PTFE powder and tilted the platform to coat the droplet with hydrophobic powder.

2.3. Measurement of the Collapse Time of Water LMs with Embedded Agarose Hydrogel

To measure the collapse time, the LM was placed on a flat substrate, and the changes in mass were recorded until the surface of the marble started to shrink and deviated from a spherical
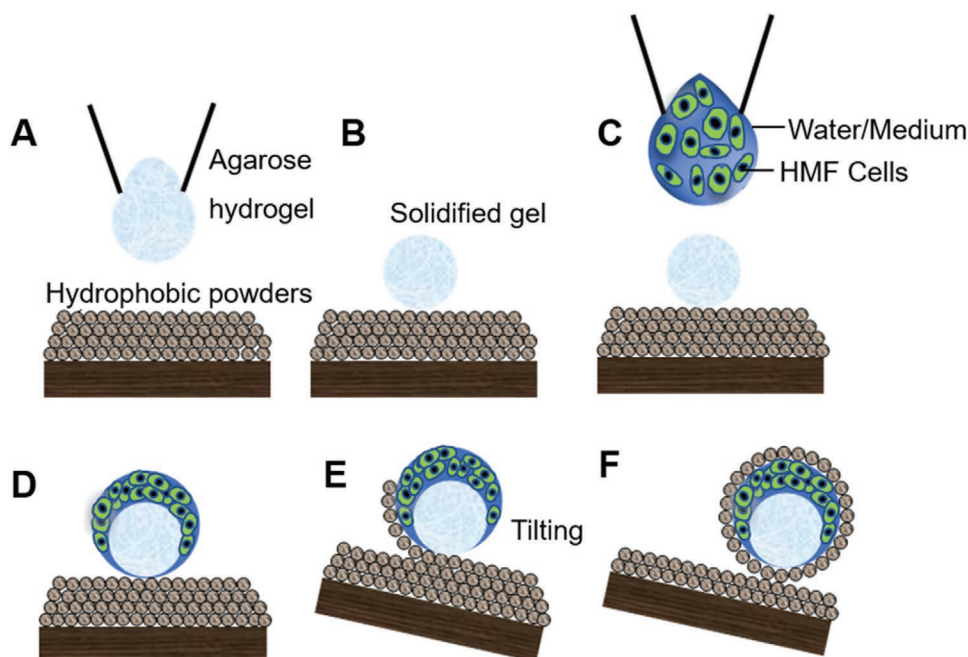
**ADVANCED
SCIENCE NEWS**

www.advancedsciencenews.com

**ADVANCED
BIOLOGY**

www.advanced-bio.com

Figure 1. Schematic illustration of the formation process of LMs with embedded agarose hydrogels by using DI water, cell culture medium (i.e., DMEM/F12), and DMEM/F12 containing HMF cells. A) First, 5 µL of agarose hydrogel solutions with different concentrations is prepared and immediately placed in a well containing hydrophobic powder. B) After 2 min in room temperature, the hydrogel becomes solidified and forms a solidified gel with spherical shape. C,D) A total of 10 µL of DI water or DMEM/F12 without cells or DMEM/F12 with HMF cells was deposited on the solidified hydrogel and formed a compound droplet. E) The platform was tilted and compound droplet was coated with PTFE hydrophobic powder (with nominal particle size of 1 µm). F) Formation of three different LMs with embedded agarose hydrogel, i.e., 1) DI water+agarose+PTFE; 2) DMEM/F12+agarose+PTFE; and 3) DMEM/F12+HMFcells+agarose+PTFE.

shape. All the measurements were conducted in an air-conditioned laboratory environment at a temperature of 21 ± 0.5 °C, 1 atm pressure, and RH of 57.3% ± 3%. The side view of the evaporating LM was recorded using a camera (EO-5012C 1/2 in. CMOS color USB camera with 1.0× telecentric lens). The camera was mounted horizontally on a motorized linear stage (Zaber Technologies T-LS28M) to adjust the focus. **Figure 2** shows the schematic view of the experimental setup.

2.4. Measurement of the Mass Loss of the Agarose-Embedded LM in Dry and Humid Incubators

To investigate the effect of agarose concentration on the mass changes of the LM with embedded agarose hydrogel, pure LMs as well as LMs with 0.25–1% embedded agarose hydrogel were prepared with water. The measurement was carried using an electronic balance that was calibrated before each run
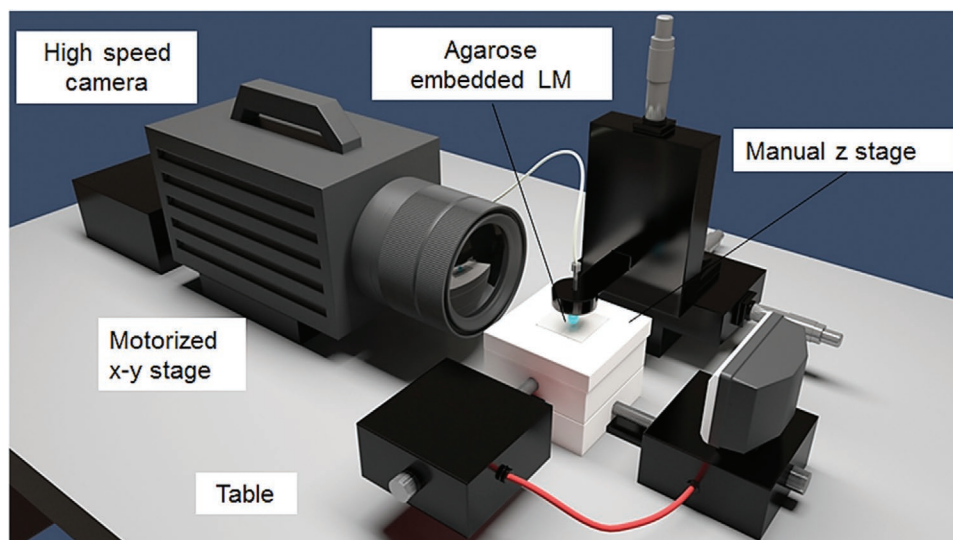

Figure 2. Schematic representation of the experimental setup to determine the collapse time of agarose-embedded LM.

and logged; the mass changes were recorded by using a USB camera at a fixed time interval of 10 min. Figure 4D shows the schematic of the experimental setup. The water absorption capacity of agarose at different concentrations (0.25–1%) was measured by isolating the gel from the LM after 15 min of incubation at room temperature, followed by measuring the weight of the agarose gel. The mass change of the LMs was measured on the weighing pan of an electronic balance fitted with a draft shield for 60 min. To evaluate the potential of agarose to absorb moisture from the surrounding environment, the mass loss was tested by exposing the LM into a dry incubator for 60 min. Then after, the LM was transferred into the humidified incubator. In both cases, the temperature of the incubator was kept constant at 37 °C. The mass change was recorded at the fixed time interval of 10 min. All the measurements were conducted under the respective environmental conditions. The humidity was monitored throughout the experiments using a humidity meter. The procedure was followed to test LM with/ without agarose and agarose gel only.

2.5. 3D Cell Culture inside the Agarose-Embedded LM

The study followed the same procedures as thoroughly explained in a previous work to culture multicellular spheroids inside the LM with embedded agarose.[13] Briefly, a 10 µL droplet containing 5×10^3 cells was injected to collide with the top of the agarose gel. HMF cells were used, which had been cultured in T25 flasks at 37 °C in a humidified incubator inclusive of 5% CO_2 in DMEM/F-12 medium with 10% FBS (Gibco, Australia #10099133) and 1% penicillin/streptomycin (Fisher Scientific; Australia, #15140122). After incubation for 24–72 h at 37 °C and humidified environment, the cell aggregated and formed spheroids inside the LM. The spheroids were then harvested by puncturing the marble with a needle, allowing the content to settle at the bottom of the well and suspend with 100 µL of the culture medium. Finally, the spheroids were examined and subjected to further characterization.

2.5.1. Qualitative Analysis of Cell Viability of the Harvested Multicellular Spheroids

In the experiments, nucleic acid binding dye and live-dead fluorescent dyes were used to stain spheroids in each experiment. Spheroids harvested from single LM were transferred into an Eppendorf tube and washed with phosphate-buffered saline (PBS). Then, it was incubated with 5 µL of acridine orange (AO; Sigma #65612) (10 µg mL^{-1}) and propidium iodide (PI; Sigma #25535164) (10 µg mL^{-1}) at a ratio of 1:1 in 1 mL of the medium for 30 min at room temperature. After the staining procedure, the spheroid was washed with PBS by centrifugation at 1000 rpm per 5 min. After centrifugation, the supernatant was removed partially, leaving ≈50 µL of the medium/pallet mixture. The pellet was gently resuspended, and 10 µL of cell suspension was pipetted on a glass slide for microscopic examination. Subsequently, the fluorescent images were obtained with a fluorescent microscope (Nikon Eclipse Ti2).

2.5.2. Quantitative Analysis of Cell Viability of the Harvested Multicellular Spheroids

The LM-containing spheroids grown at desired time points were merged with 10 µL droplet of CellTiter-Glo 3D reagent (Promega #G9682) on "U"-bottomed 96-well opaque culture plate. Then after 30 min, the luminescent signal intensity was detected using a SpectraMax plate reader.

2.5.3. Glucose and Lactate Quantification

After 48 h of incubation, the cell culture media inside the LM was collected to quantify the extracellular glucose and lactate production. The collected culture media was centrifuged at 1000 rpm per 3min. After centrifugation, the supernatant was retrieved and further analyzed for glucose and lactate concentration using a BD-7D bioanalyzer (Oji Scientific, Japan).

2.5.4. Effect of Serum Release on Spheroid Formation

For serum release study, 5 µL of 0.5% agarose solution was mixed with FBS. Subsequently, 10 µL of cell suspension was immersed onto the FBS-loaded agarose to generate a compound LM. To track the spheroid formation inside agarose-embedded LM, the cells were stained with fluorescent CellTracker Green CMFDA dye (Invitrogen # C2925) with emission/excitation wavelength 492/517 nm. The spheroid formation in 48 h was imaged using an FV3000 confocal microscope (Olympus, Japan). The fluorescent images from each observed condition were obtained.

2.6. Statistical Analysis

The results were expressed as the mean with a standard error of mean (SEM). All quantitative values were performed at least three times. The number of samples for mass loss was $n = 9$ LM, cell viability $n = 6$ LM, glucose and lactate $n = 6$ LM, and serum release study $n = 6$ LM. Statistical significance was analyzed using a one-way analysis of variance (ANOVA) with Bonferroni multiple comparison tests. The differences were significant when $p < 0.001$. Graphs were plotted using GraphPad Prism 5 software.

3. Mathematical Modeling and Numerical Simulation

A new multiphysics mathematical model of the LM coated with PTFE powder was established to elucidate the effect of environmental conditions, marble-coating, and hydrogel concentration on the evaporation of the water content. A finite element method was used to discretize and solve the coupled governing equations of moist air as ambient environment, liquid water as free-flow domain, and agarose hydrogel as a porous media domain. The evaporation-induced ablation phenomenon is also modeled to dynamically simulate LM evaporation (LME) and to calculate the collapse time of the LM.
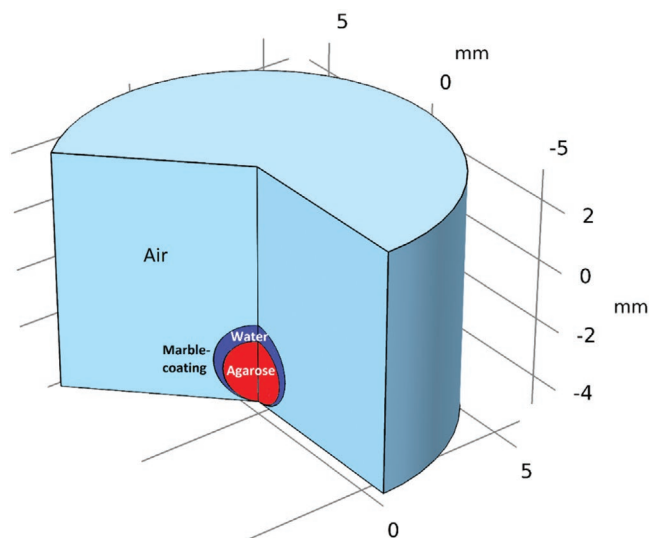
**ADVANCED
SCIENCE NEWS**
www.advancedsciencenews.com

**ADVANCED
BIOLOGY**
www.advanced-bio.com

Figure 3. Computational domain of the proposed LME model.

3.1. Computational Domain

To simulate the mathematical model of LM, a 2D axisymmetric computational domain with the same dimensions as the experimental setup was used. **Figure 3** shows the three different regions of the computational domain, including 1) moist air with RH of 57.3% (cylindrical far-field shown in pale blue); 2) liquid water droplet with 10 μL volume (free-flow domain shown in dark blue); and 3) hydrogel with different agarose concentrations (0.25%, 0.5%, and 1%) and 5 μL volume (the porous medium is shown in red). The marble-coating is assumed as a barrier between the water droplet and air. The LM droplet is supposed to be located on a horizontal surface with a 180° contact angle.

3.2. Governing Equations

3.2.1. Fluid Dynamics

The Navier–Stokes and Brinkman equations were used to calculate the flow fields of a water droplet as an incompressible and Newtonian fluid as well as an agarose droplet as a porous media perfused by water, respectively. This flow is a gravity-driven creeping type. Therefore, the Navier–Stokes equation is reduced to the Stokes equation with pressure, gravity, viscous, and transient terms (Equation (1)). The Brinkman equation of hydrogel with negligible Forchheimer drag and without any mass source is derived in Equation (2). It should be noted that Brinkman equations are modified forms of Darcy's law where one can impose the boundary conditions at the interface between a porous medium and an open fluid domain. Brinkman assumed large porosity for porous media to compare the law with experimental data. The only difference between Brinkman and Darcy's equations is the viscosity term $\nabla \cdot (\mu(\nabla u + (\nabla u)^T))$. Since hydrogel is a porous domain with large porosity, Brinkman's law is a better choice than Darcys' law. The viscosity term of Brinkman's equations depends on the

shear rate that is considerable for large porosity domains. This term can be considered to model both Newtonian and non-Newtonian fluids. In addition, Brinkman's equations are more suitable for a porous medium that has an interface with free-flow liquid. Such conditions are valid for an agarose droplet perfused with water. According to Equation (3), the continuity equation of incompressible liquids is applied to both free-flow water and porous agarose without any additional mass sources

$$\rho \frac{\partial u}{\partial t} = \nabla \cdot \left[-pI + \mu \left(\nabla u + (\nabla u)^T \right) \right] + \rho g \tag{1}$$

The Brinkman equation of hydrogel without any mass source and negligible Forchheimer drag is

$$\rho \frac{\partial u}{\partial t} = \nabla \cdot \left[-pI + \frac{\mu}{\varepsilon_h} \left(\nabla u + (\nabla u)^T \right) \right] - \frac{\mu}{k_h} u + \rho g \tag{2}$$

$$\nabla \cdot u = 0 \tag{3}$$

where u is flow velocity vector; p is the flow pressure field; μ and ρ are, respectively, the dynamic viscosity and density of water; g is gravitational acceleration; and ε_h and k_h are porosity (set to be 0.9[23]) and permeability (set to 367 nm^2[23]) of the agarose hydrogel, respectively. The compressible flow equations can be also applied to the moist air, far-field, if ambient flows are existing.

3.2.2. Concentration

The agarose in the water liquid phase is not adsorbed onto the surface of the porous hydrogel. Therefore, the convection–diffusion equation was applied to calculate agarose concentration in both porous hydrogel and free-flow water droplet[19]

$$\frac{\partial c_{aga}}{\partial t} + \nabla \cdot \left(u c_{aga} \right) = D_w \nabla^2 c_{aga} \tag{4}$$

$$\frac{\partial \left(\varepsilon_h c_{aga} \right)}{\partial t} + \nabla \cdot \left(u c_{aga} \right) = D_h \nabla^2 c_{aga} \tag{5}$$

D_h and D_w are, respectively, diffusion coefficients of agarose in hydrogel and water assumed to be the same and equal to 10^{-11} m^2 s^{-1}[24] and c_{aga} is the agarose concentration.

3.2.3. Evaporation

The vapor concentration equation was applied to determine the moist air condition of the surrounding environment of LM

$$\frac{\partial \left(M_v c_v \right)}{\partial t} + u_a \cdot \nabla \left(M_v c_v \right) = D_a \nabla^2 \left(M_v c_v \right) \tag{6}$$

In the above equation, $c_v = \phi c_{sat}$, where c_v is the vapor concentration related to RH (ϕ) and the vapor saturation concentration ($c_{sat} = 0.96$ mol m^{-3}). Also, D_a is the water vapor diffusion

**ADVANCED
SCIENCE NEWS**
www.advancedsciencenews.com

**ADVANCED
BIOLOGY**
www.advanced-bio.com

coefficient in the air (2.6×10^{-5} m^2 s^{-1}), M_v is the molar mass of water vapor (0.018 kg mol^{-1}), and u_a is the airflow velocity that is set to zero based on the no-flow condition of the experiment setup.

3.3. Initial and Boundary Conditions

3.3.1. Fluid Dynamics

Initial velocity and pressure fields are assumed to be zero in both water droplet and hydrogel porous media. No-slip boundary condition is applied on the LM droplet surface.

3.3.2. Concentration

The initial concentration of agarose is selected to be zero for the water droplet and c_0 (set by different values; 6.5, 13, and 26 mol m^{-3}) for the hydrogel. The continuity boundary condition for the hydrogel–water interface and impermeable barrier boundary conditions for the water–air interface were also applied. The discontinuity flux boundary condition was set at the interface of water and the horizontal bottom. No-flux boundary condition was utilized for the far-field boundaries.

3.3.3. Evaporation

The standard pressure and temperature conditions are chosen for the moist air, far-field. Initial RH is assumed to be 57.3%, and initial liquid water concentration on the moist surface of the water droplet, $c_{l,init} = 38.14$ mol m^{-3}. The insulation boundary condition is applied for the horizontal bottom, and the other boundaries of the air domain, right and top boundaries in Figure 3, are set to a constant RH of 57.3%. As evaporation inhibition effect of the bottom surface, insulation condition is also applied to the contact surface of the LM and the horizontal bottom.

3.4. Evaporation Rate of Pure Water Droplets

The evaporation rate on the water droplet surface as the main model parameter was modeled by coupling Equations (7) and (8), respectively, describing evaporation flux and changing liquid water concentration of moist surface

$$-n \cdot f = f_{evap} = \begin{cases} M_v K (c_{sat} - c_v) & \text{if } c_v > c_{sat} \text{ or } c_l > 0 \\ 0 & \text{otherwise} \end{cases} \quad (7)$$

$$M_v \frac{\partial c_l}{\partial t} = -f_{evap}, c_l(0) = c_{l,init} \quad (8)$$

where f is the evaporation flux, K is the evaporation rate, c_l is the liquid water concentration on the moist surface, and n is the normal unit vector of the moist surface. According to $c_v = \phi c_{sat}$, the evaporation flux, Equation (7) can be rewritten as

$$f_{evap} = \begin{cases} M_v K c_{sat} (1 - \varphi) & \text{if } c_v > c_{sat} \text{ or } c_l > 0 \\ 0 & \text{otherwise} \end{cases} \quad (9)$$

Therefore, according to Equation (9), increasing RH decreases the evaporation rate, which is in agreement with our experimental observations. In this model, we consider two natural constrains on the evaporation process. First, based on Equation (8), liquid water concentration cannot be a negative value. Second, Equation (9) indicated that the evaporation process stops when the surrounding air becomes saturated, i.e., $\phi = 1$.

3.5. The Effect of the Coating Particles on the Evaporation Rate of LMs

In addition to the RH as an environmental condition, the coating layers of the hydrophobic powder also affect the evaporation rate of LM.[25] Therefore, by comparing the evaporation rate of a pure water droplet with an LM, we derive a new empirical equation for the evaporation rate. This part of the model is based on the evaporation resistance caused by the marble-coating.[6,25] The empirical equation describing the evaporation rate of an LM (without hydrogel), $K_{LM}(\phi)$, which takes into account the effect of the covering small particles on the evaporation rate, is presented in Equation (10)

$$K_{LM}(\varphi) = K_0(\varphi) e^{-(0.01 R(\varphi))} \quad (10)$$

where $K_0(\phi)$ is the evaporation rate of a pure water droplet as a function of RH and $R(\phi)$ is evaporation resistance as a result of PTFE coating. It should be noted that the evaporation resistance is related to the difference between evaporation rates of pure water and LM droplet.[25] These empirical functions, $K_0(\phi)$ and $R(\phi)$, are, respectively, derived as Equations (11) and (12)

$$K_0(\varphi) = -3 \times 10^{-7} \varphi^2 + 1 \times 10^{-8} \varphi + 2 \times 10^{-7} \quad (11)$$

$$R(\varphi) = 35.643 \varphi^2 + 15.17 \varphi + 34.521 \quad (12)$$

Equations (10)–(13) were derived through curve fitting of RH-evaporation rate profiles of water and marble droplets, using the experimental data of both Tosun and Erbil[25] and our experimental results for LM without agarose.

3.6. The Effect of Agarose Concentrations on the Evaporation Rate of LMs with Embedded Hydrogel

In addition to the RH and coating layers, the concentration of agarose hydrogel also affects the evaporation rate. Accordingly, by comparing the evaporation rate of pure LM with that of LMs with embedded hydrogels of different agarose concentrations, we expand the empirical equation of evaporation rate to a more general equation that can determine

the evaporation rate of any types of droplets, i.e., pure water, pure LM, and LM with an embedded hydrogel with different agarose concentrations

$$K_{\text{LMA}}\left(\varphi, c_{\text{aga}}\right) = K_{\text{LM}}\left(\varphi\right) \beta\left(c_{\text{aga}}\right) \tag{13}$$

where $K_{\text{LMA}}(\phi, c_{\text{aga}})$ is the evaporation rate of an LM with embedded agarose hydrogel, and $\beta(c_{\text{aga}})$ is a normalized function defining the increment of the evaporation rate due to the agarose concentration that can be calculated from the following equation

$$\beta\left(c_{\text{aga}}\right) = 6.53 \times 0^{-2} c_{\text{aga}}^2 + 9.33 \times 10^{-2} c_{\text{aga}} + 1 \tag{14}$$

Equation (13) was derived from curve fitting of experimental evaporation rates of LMs with embedded agarose of different concentrations. Indeed, β in Equation (13) is a correction factor to modify Equation (10), i.e., the evaporation rate of LM. This approach allows for modeling of the evaporation of LMs with embedded agarose.

3.7. The Effect of Ablation on the Collapse Time of LMs with Embedded Hydrogel

The surface evaporation causes ablation from the outer surface of the LM with a rate equal to the empirically calculated evaporation rate, Equation (14). We mathematically modeled the ablation process to reasonably calculate the collapse time when the droplet loses its spherical shape. We used the collapse time as a characteristic parameter of the LME model. The surface ablation rate, $V_{\text{ab}}(\phi, c_{\text{aga}})$, is derived as

$$V_{\text{ab}}\left(\varphi, c_{\text{aga}}\right) = K_{\text{LMA}}\left(\varphi, c_{\text{aga}}\right) \delta\left(b\right) \tag{15}$$

where $\delta(b)$ is a step function that describes the inhibition effect of the horizontal bottom as a rigid surface on the deformation of LM.

3.8. Numerical Implementation

The obtained mathematical models, including the fluid dynamics equations of free-flow and porous media, the concentration equations of agarose into both porous hydrogel and free-flow water droplet, and the evaporation–ablation-coupled equations were computationally implemented in COMSOL Multiphysics version 5.3. For solving the transient equations, PARDISO direct nonlinear solver was utilized. The initial and maximum time steps were set 0.001 and 0.1 s, respectively. Three numbers of triangular linear elements equivalent to 6497, 8122, and 9746 were applied to consider mesh independency. The mesh with 8122 triangular elements was specified to arrive a mesh-independent and cost-effective computational setup in terms of both flow and concentration equations.

4. Results and Discussion

4.1. Experimental Section

4.1.1. Evaporation Rate of Agarose-Embedded LM in Room Temperature

Figure 4A depicts the evaporation process of LM with an embedded hydrogel sphere of different agarose concentrations. The control is a pure LM without hydrogel. Other LMs contain a liquid volume of 10 µL and a hydrogel with a volume of 5 µL. As can be seen from Figure 4A, the LMs with embedded hydrogels can retain their spherical shape for a longer time compared to a pure LM without hydrogel (control). In addition, the evaporation rate seems to be a function of the agarose hydrogel concentration (Figure 4B). The mass change profile of LM containing agarose gel at the concentration of (1–0.25%) showed a significantly slower evaporation rate compared to control. However, we did not observe any significant changes within groups of these concentrations (1–0.25%). The survival of LMs containing agarose could be assigned to the water absorbed by the agarose gel. The agarose polymer is porous. The pores provide stronger binding sites with water molecules and exhibit a higher water holding capacity. The porous nature is governed by the concentration of agarose. As the concentration of the agarose decreases, we expected that its porosity increases,[26] considerably retain more water. We investigated the behavior of water absorption capacity in three different concentrations of agarose, namely 0.25%, 0.5%, and 1% agarose marble, respectively. The water absorption was higher in 0.5% agarose than 1% agarose. Conversely, water absorption of 0.25% agarose was significantly lower (Figure 4C). At a concentration of 0.25%, due to the highly porous nature, the water content is saturated. Thus, further water absorption is not possible. This observation suggests that 0.5% agarose is optimal for maintaining slower evaporation inside LM. It is probable that at a humidified environment, 0.5% agarose facilitates water molecules uptake from surrounding moisture which diffuses through the liquid–air interface into the LM.

4.1.2. Effect of RH and Agarose Hydrogel on Evaporation of LM

We postulate that agarose gel absorbs water molecules from the humid environment and retains water. The possibility of the agarose gel to resist evaporation was evaluated by recording the mass change in LM containing 0.5% agarose and cell culture medium (now abbreviated to as LMA) at the same condition as that of the cell culture. We first investigated the mass changes at different RH values. We found that LM suffered a rapid mass loss in a duration of 60 min when exposed to 37 °C in a dry incubator (where the RH was around 40%) (**Figure 5**A). As expected, LMA showed a reduced mass loss in a humidified incubator (where the RH was around 85%). However, the LM continued to suffer from evaporation (Figure 5B). In another set of experiment, marbles were initially exposed to a dry incubator for 60 min and then transferred to the cell culture incubator with the RH ≈85% for another 60 min. The mass loss was recorded at intervals of 10 min. This experiment was

ADVANCED
SCIENCE NEWS
www.advancedsciencenews.com
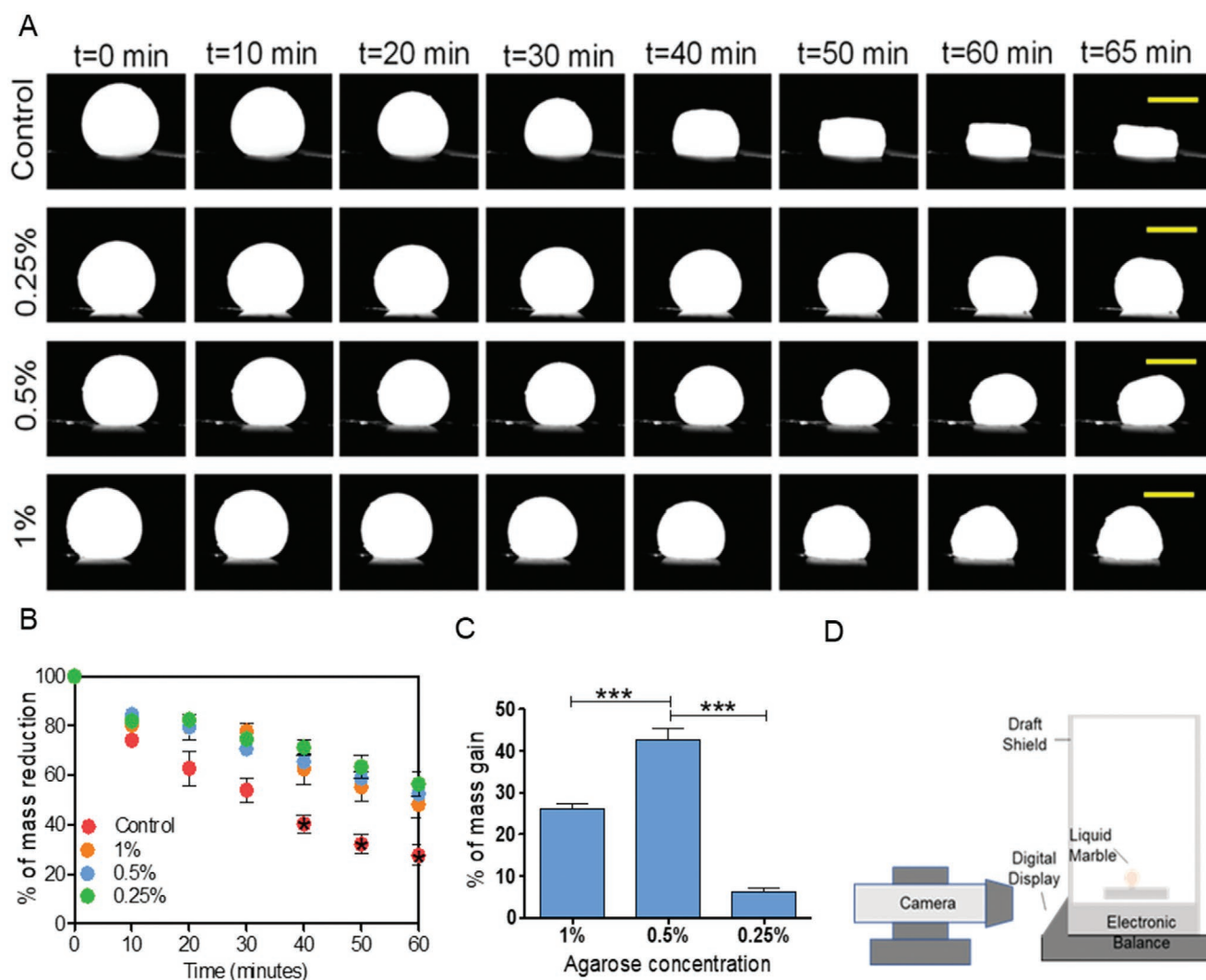
ADVANCED
BIOLOGY
www.advanced-bio.com

Figure 4. The evaporation process of the LM with an embedded hydrogel of different agarose concentrations. A) Horizontal profile of volume loss in LM. B) Mass loss in LM embedded with agarose at the concentration of 0.25–1%. The control is a pure LM without hydrogel. Student's *t*-test analyses showed that there was significantly more mass loss in control (*$p < 0.05$). C) Water absorption capacity of agarose hydrogel at different concentration. One-way ANOVA was performed to determine the significance of differences, followed by a Bonferroni test. Statistical significance: ***$p < 0.001$. D) Schematic of the experimental setup. All experiments were repeated three times. Bars represent the mean; error bars represent the standard error of the mean ($n = 6$ LM). Scale bar 2000 μm.

carried out to elucidate the ability of marbles to regain its mass by absorbing moisture from the surrounding environment. Interestingly, a constant LMA evaporation rate was recorded. It appears that the evaporation rate in LMAs was significantly slower, with almost no further mass loss. Lastly, we investigated the role of the agarose gel in the evaporation process. The agarose gel absorbed water from the surrounding humid environment and showed a recovery trend by absorbing moisture (Figure 5C). As depicted in Figure 5Div–vi, the LMA was found to retain their shape to approximately spherical geometry when an equilibrium state of absorption and evaporation was reached. In contrast, the pure LM showed a reduction in mass, about ≈20% and unable to hold its spherical shape and undergo dramatic deformation such as buckling (Figure 5Diii). As the buckling commences, the PTFE powder becomes dense, and a void at the air–water interface will be formed. It is thus,

possible that the buckling LM becomes less hydrophobic and possibly allow water molecule to diffuse via evaporation. Consequently, buckling LM undergoes catastrophic evaporation and fails to retain water to regain spherical shape. Overall, the observations suggest that the gel inside the LM may act as a source to absorb water molecules in the air and retain water inside the LM. Interestingly, the gel did not show a massive mass loss. Possibly the gel retains water and maintains its volume when exposed to humidified surrounding (Figure 5Dvii–xi).

4.1.3. Evaporation Rate of Agarose-Embedded LM Containing Cells inside the Humidified Incubator

The LM is a unique and reliable platform for liquid handling and manipulation. In the previous study, we also demonstrated
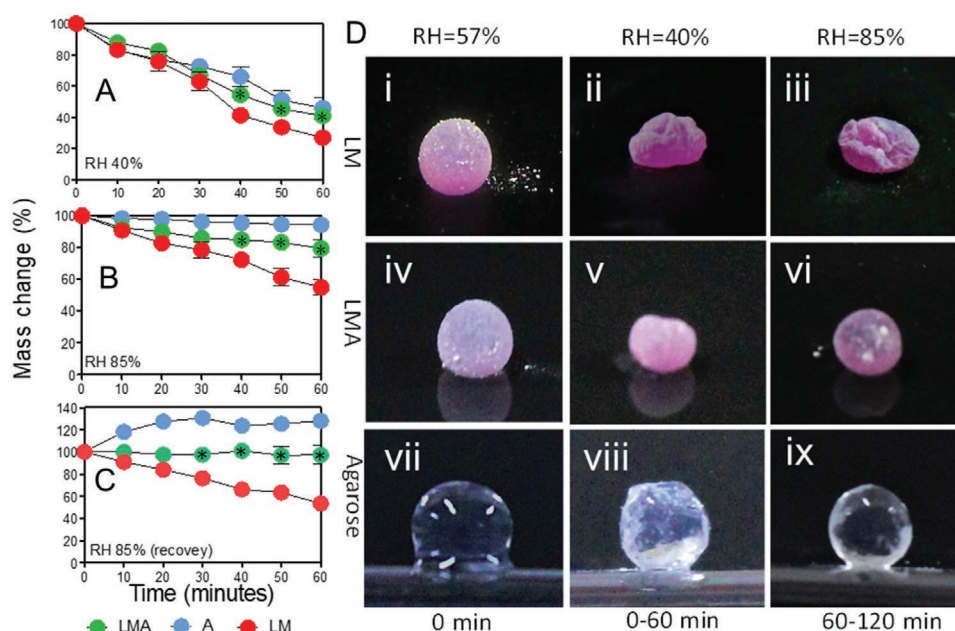
Figure 5. Effect of RH and agarose hydrogel on evaporation of LM. A) Changes in mass as a function of at RH = 40% and B) at RH = 85%. C) LMs were first incubated inside a dry incubator with RH = 40% for 60 min and then transferred to a humidified incubator (RH at ≈85%) for another 60 min (abbreviated as recovery). The percentage of the mass changes (loss or gain) was calculated at intervals of 10 min. Student's *t*-test analysis was performed. Statistical significance: *$p < 0.01$. Results of triplicate experiments. Error bars represent the standard error of the mean ($n = 9$ LM). D) Qualitative illustration of morphological change of the marbles and the gel at the initial phase of sample preparation (0 min), followed by dry incubator (0–60 min) and finally at humidified incubator (60–120 min). Images represents: i–iii) LM; iv–vii) LMA; and vii–ix) agarose gel. The scale bar is 1000 µm.

that FLM minimizes evaporation and was useful for growing cell spheroids.[13] In a floating system, the coating layer of LM and surface of the liquid bath is detached with a thin air pockets layer, this interface facilitates the absorption of water molecule into the LM and subsequently reduces the loss of mass due to the evaporation process. However, we found that FLM presents certain drawbacks, such as stability and dispensability. They are fragile and easily broken. In this regard, a sessile LM will be more reliable for liquid handling. Thus, we aim to develop a stable sessile LM that potentially can extend the culture period for 3 days. As mentioned before, evaporation of biological fluid in the culture medium may not be favorable for extended incubation periods. Under these conditions, the fluid loss causes medium components to concentrate and followed by precipitation of protein.[27] These negatively impact the growth condition by affecting the essential factors for spheroid growth such as 1) osmotic stress in cells and cell volume changes[28] and 2) supply of metabolites to the cells[29] and waste from cells may not be efficiently removed. Interestingly, all the above experiments have yielded consistent results for the effects of evaporation under normal atmospheric conditions. The LM with embedded agarose sustains the morphology of LM and reduces the loss of vapor. This existing observation motivates to tailor the application of LM with embedded agarose for culturing cells. Thus, we investigate the behavior of LM with embedded agarose with biological cells in a humidified environment at 37 °C. These useful insights of LM with embedded agarose may further apply to minimize evaporation and allow ideal spheroid growth conditions through incubation using a humidified atmosphere. The spheroids grown from the HMF cell lines have been classified into two LM groups

depending upon the presence of agarose. Our result confirms that utilizing agarose hinders the evaporation rate. The LM filled with agarose maintains its spherical shape. However, a small loss of liquid is noticeable after 72 h, which can be interpreted by marble shrinkage and volume loss (**Figure 6**).

In contrast, cells grown without agarose gel showed a gradual increase in wrinkle formation on the hydrophobic coating and lost their spherical shape within 24 to 72 h. Next, we broke the LMs to harvest the spheroids and investigated the cell viability at 24, 48, and 72 h. The spheroid vitality status was assessed qualitatively by staining with fluorescent dyes AO and PI. This
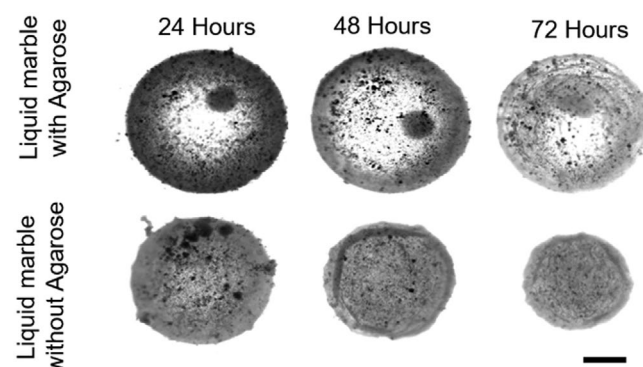

Figure 6. Brightfield images showing the bottom view of the LM during evaporation at 37 °C. The LM was incubated inside a humidified CO_2 incubator (the images were taken at room temperature). The evaporation effect constitutes shape transformation with the eventual shrinking and volume loss. Scale bar 500 µm.
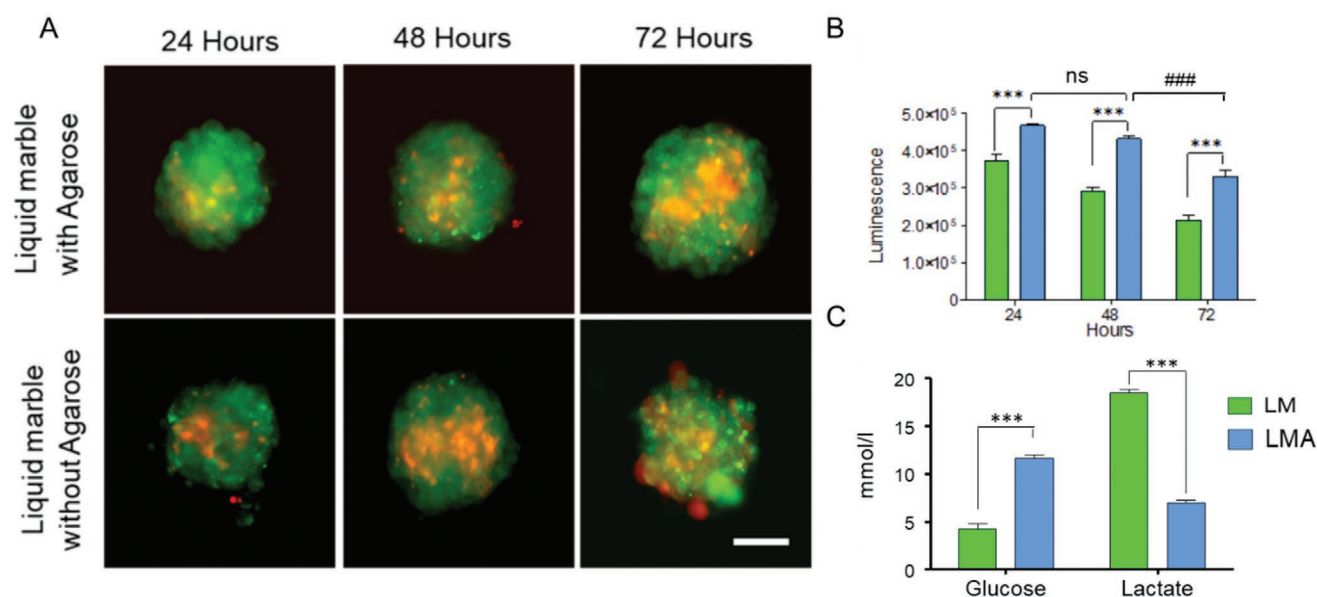
Figure 7. Effect of evaporation on spheroid viability. A) Qualitative comparison of cell viability: representative images of combined fluorescence of AO and PI staining for 3D spheroid harvested from LM with and without embedded agarose gel at 24, 48, and 72 h incubation time. AO and PI show the presence of live (green) and dead (red) cells. The samples show a gradual increase in the necrotic centre with the PI staining over time. A lower number of PI-positive cells are observed in spheroids grown inside LM filled with agarose. Scale bar 50 µm. B) Quantitative comparison of cell viability: The viability of the spheroids was measured by using the CellTiter-Glo 3D Cell Viability assay. Bar graph showing a significant reduction in luminescence in spheroids that were harvested from LM without agarose at each incubation time. The plots show that the reduction in the spheroid viability in the LM with agarose correlates directly to the incubation time. The viability of spheroids derived from LM containing agarose did not lead to a significant decrease between 24 and 48 h. C) Quantification of extracellular glucose and lactate production. Data were analyzed using one-way ANOVA followed by post hoc Bonferroni's test. Statistics: $***p < 0.01$, $###p < 0.01$, and ns = not significant. All experiments were repeated three times. Results of triplicate experiments are shown with error bars, representing mean $\pm$ SEM ($n = 6$ LM). The scale bar in (A) is 50 µm. LMA, LM with agarose hydrogel.

staining method gives a realistic view of live/dead cell distribution and indicates the time when necrosis starts to increase. We noticed that the radius of the necrotic core increased significantly from 24 to 72 h in the absence of agarose gel (**Figure 7**A). However, a lack of quantitative measure presents due to the irregular size of the necrotic core area in the spheroid.

To further strengthen the data, we performed a quantitative cell viability assay to present a more accurate assessment of all the cells within a spheroid. The viability of the spheroid harvested from LM with embedded agarose was also affected by evaporation. However, we noticed that there was a significant drop in cell viability ($p < 0.001$) in groups without agarose at all time points (Figure 7B). Accordingly, both tests signify that LM with the presence of agarose greatly contributes to minimizing evaporation and improves cell viability. The loss of small volumes of fluid causes culture media to become concentrated and elevates osmolarity. This alters cell permeability and impairs normal cell physiology. Eventually, metabolic waste accumulates and triggers necrotic death of cells at the center of the spheroid. The LM-containing agarose circumvents rapid evaporation rate. Interestingly, we found that the LM-containing agarose showed a reduction in lactate production and increase glucose consumption at 48 h of culture (Figure 7C). Lactate is a metabolic waste that could increase the condition of oxidative stress and cause perturbations in cellular function. However, the quantitative understanding of the relationship between evaporation, oxygen level and lactate production is not known. This observation provides a hint that prevention of evaporation can potentially reduce metabolic waste

accumulation, and also increase glucose consumption, thereby maintains the appropriate necessary condition for optimal cell growth. Thus, it maintains natural 3D microenvironment to avoid the osmotic shift of extracellular fluid that may negatively impact cell viability. The spheroids grown in LM with embedded agarose did not trigger necrosis at the innermost core of the spheroid. It should be noted that in the present work, we did not use hydrogels as an extracellular matrix (ECM) for the cells that may act synergistically to promote cell–cell and cell–matrix interactions. Additionally, in this study, as a proof of concept, we loaded agarose with FBS inside LM to function as a slow-release carrier (**Figure 8**). The release FBS from the agarose gel into the surrounding cell suspension yields multiple spheroid growths in LM-containing gel (Figure 8iii,vi). In contrast, irregularly shaped aggregates are formed in LM without gel (Figure 8i,iv). This concept provides an advantage of increasing the potency of growth factors and maintaining their bioactivity for an extended period. Hence, the role of agarose predominantly functions to reduce the evaporation rate and facilitate 3D spheroid growth.

4.2. Theoretical Section

4.2.1. Verification of the Mathematical Modeling and the Numerical Simulations

In Section 3, we obtained a coupled mathematical model based on the derived empirical equations that can predict the
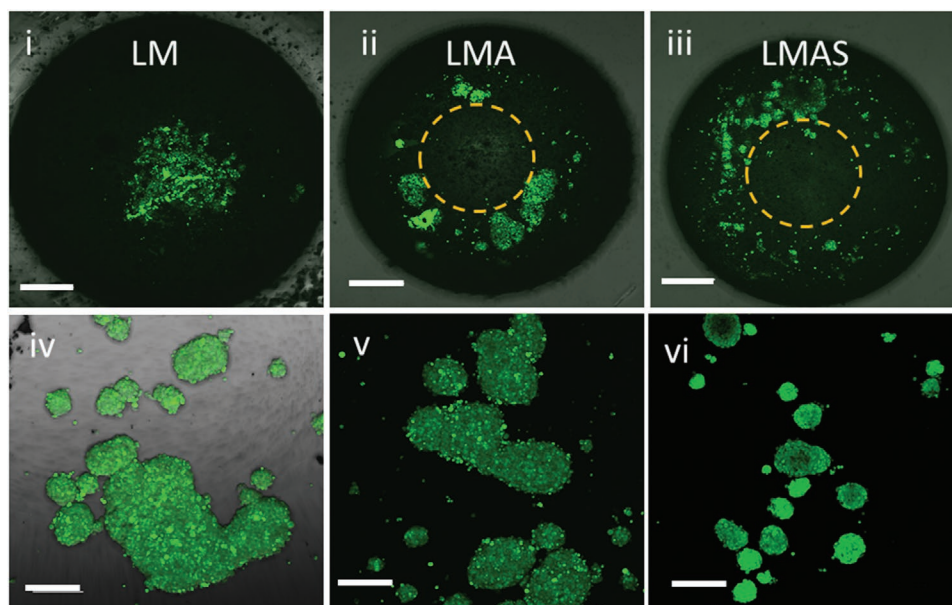
Figure 8. Effect of serum release on spheroid growth. The bottom view of LM depicts spheroid formation after 48 h of incubation was compared with i) control (LM without agarose); ii) LM with agarose; and iii) LM containing agarose loaded with serum. All LMs contain cells at a seeding density of 500 cells μL⁻¹. iv–vi) The LMs were broken and spheroids allowed to settle to the bottom of the well. The orange circle indicates the location of the agarose sphere. Scale bar for (i–iii) is 500 μm and for (iv–vi) is 200 μm. LMA, LM with agarose hydrogel; LMAS, LM with agarose hydrogel loaded with serum.

evaporation rate and collapse time of an LM with embedded agarose hydrogel. To verify the validation of this model, the numerically calculated collapse times for different agarose concentrations are compared to those obtained from the experimental data (average of four experiments) (**Figure 9**). According to these results, the coupled mathematical model, which was based on evaporation-induced deformation of LM droplet, (Equation (15)), can calculate the collapse time of LMs with embedded agarose hydrogels with an error of less than 10%. Therefore, this new mathematical model can be applied to any type of liquid droplets, i.e., pure liquid droplet ($R(\varphi) = 0$, $c_{aga} = 0$), LM droplet ($c_{aga} = 0$), and LM droplet including hydrogel with different agarose concentration.
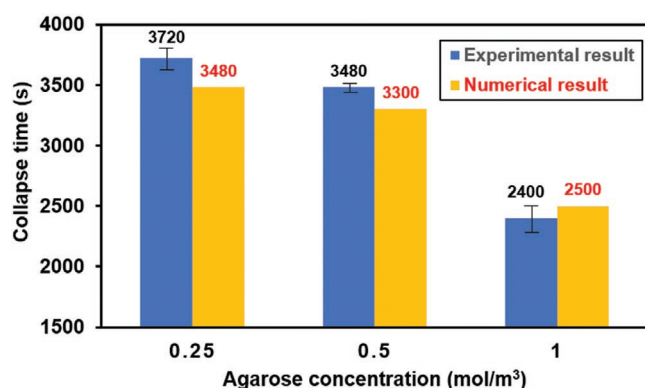

Figure 9. Verification of the numerical results: The numerically calculated values of the collapse time of LM droplet with different agarose concentrations compared to those of experimental results. The values of the experimental results are the average of four experiments with corresponding error bars. The proposed model can predict the collapse time of LMs with less than 10% error.

4.2.2. The Distributions of Agarose Concentration and Vapor Concentration in LMs with Embedded hydrogel

Agarose Concentration: The concentration distributions of 1% agarose (26 mol m⁻³) after 100 s from the initial condition and 2500 s as the collapse time are shown in **Figure 10**A. As shown in the collapsed droplet, agarose is concentrated at the bottom areas of the LM and is beneficial for toroidal cell culture[13] and agrees well with the experimental observations. It is noteworthy that this typical concentration as a result of flow-concentration coupling can also relate the evaporation rate to the hydrogel porosity. The numerically calculated collapse time of 2500 s is in a good agreement with the experimentally measured one with an error of only 4.2%.

Vapor Concentration: The relative vapor concentrations on LM surface with 1% agarose after 100 s (labeled as spheroidal) and after 2500 s (labeled as collapsed) are, respectively, shown in Figure 10B. According to this result, the maximum vapor concentration occurs at the bottom areas, where the agarose concentration and, consequently, the evaporation rate are maximum. The high evaporation rate at the bottom can increase the contact angle.

5. Conclusion

LMs are emerging microfluidic platforms that can be utilized in various applications. In contrast to the FLMs, sessile LMs suffer from rapid evaporation. In this article, we showed that embedding agarose hydrogels inside the LMs could significantly slow down the evaporation and increase their collapse time. To this aim, we experimentally investigated and compared the evaporation rate and collapse time of LMs with and without agarose hydrogel (with different concentrations). We considered
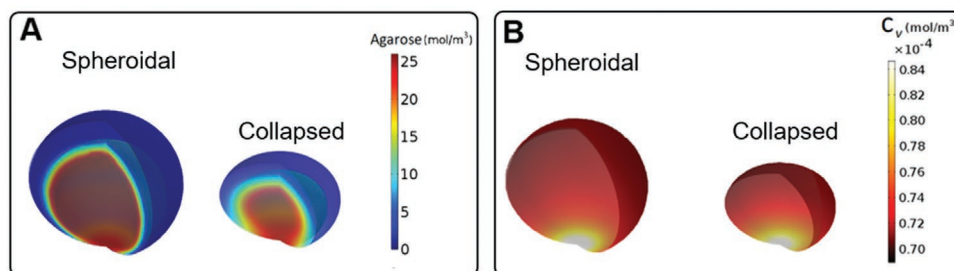
Figure 10. A) Agarose hydrogel concentration and B) vapor concentration distributions of spheroidal (after 100 s) and collapsed (after 2500 s) LM with 1% agarose hydrogel.

the evaporation rate of such LMs under three ÷ environmental conditions: 1) outside the incubators ($T = 21\ °C$, RH = 57%), without biological cells; 2) inside both dry (RH = 40%) and humid incubators (RH = 85%) at $T = 37\ °C$, without biological cells; and 3) inside the humid incubators with biological cells. In all these conditions, we observed that the embedded agarose hydrogel could significantly improve the lifetime of LMs. Furthermore, it was confirmed that the LM with embedded agarose as a microbioreactor could minimize the evaporation rate and allow the ideal growth of multicellular spheroids through incubation in a humidified atmosphere. Finally, we established a mathematical model of the LM under evaporation-induced ablation to calculate the evaporation rate of different types of LMs, including pure water and LM embedded hydrogels with varying concentrations of agarose. It was shown that the proposed computational approach could predict the collapse time of LMs with different agarose concentrations with less than 10% error.

Taken together, the proposed methodology functions as an alternative model for FLM to reduce evaporation, an ideal microbioreactor for improving spheroid growth. Additionally, it is also suitable for the development of an automated system that facilitates high-throughput replacement of culture media. Finally, we proposed a simple computational model to estimate the collapse time of LMs as a function of agarose concentrations.

Conflict of Interest

The authors declare no conflict of interest.

[1] P. Aussillous, D. Quéré, *Nature* **2001**, *411*, 924.
[2] E. Bormashenko, *Langmuir* **2016**, *33*, 663.
[3] a) C. H. Ooi, E. Bormashenko, A. V. Nguyen, G. M. Evans, D. V. Dao, N.-T. Nguyen, *Langmuir* **2016**, *32*, 6097; b) P. Aussillous, D. Quéré, *J. Fluid Mech.* **2004**, *512*, 133.
[4] U. Cengiz, H. Y. Erbil, *Soft Matter* **2013**, *9*, 8980.
[5] a) J. Tian, T. Arbatan, X. Li, W. Shen, *Chem. Eng. J.* **2010**, *165*, 347; b) J. Dobson, M. Taylor, *Electrochim. Acta* **1986**, *31*, 231.
[6] G. Barnes, *Adv. Colloid Interface Sci.* **1986**, *25*, 89.
[7] D. Zang, Z. Chen, Y. Zhang, K. Lin, X. Geng, B. P. Binks, *Soft Matter* **2013**, *9*, 5067.
[8] K. Lin, R. Chen, L. Zhang, W. Shen, D. Zang, *Adv. Mater. Interfaces* **2019**, *6*, 1900369.
[9] M. Dandan, H. Y. Erbil, *Langmuir* **2009**, *25*, 8362.
[10] M. D. Doganci, B. U. Sesli, H. Y. Erbil, B. P. Binks, I. E. Salama, *Colloids Surf. A* **2011**, *384*, 417.
[11] R. K. Vadivelu, H. Kamble, J. A. M. Shiddiky, N.-T. Nguyen, *Micromachines* **2017**, https://doi.org/10.3390/mi8040094.
[12] T.-M. Achilli, J. Meyer, J. R. Morgan, *Expert Opin. Biol. Ther.* **2012**, *12*, 1347.
[13] R. K. Vadivelu, C. H. Ooi, R.-Q. Yao, J. T. Velasquez, E. Pastrana, J. Diaz-Nido, F. Lim, J. A. Ekberg, N.-T. Nguyen, J. A. St John, *Sci. Rep.* **2015**, *5*, 15083.
[14] A. Munaz, R. K. Vadivelu, J. A. S. John, N.-T. Nguyen, *Lab Chip* **2016**, *16*, 2946.
[15] R. K. Vadivelu, H. Kamble, A. Munaz, N.-T. Nguyen, *Biomed. Microdevices* **2017**, *19*, 31.
[16] G. Pennarossa, S. Ledda, S. Arcuri, F. Gandolfi, T. A. L. Brevini, *J. Visualized Exp.* **2020**, *162*, e61655.
[17] T. A. L. Brevini, E. F. M. Manzoni, S. Ledda, F. Gandolfi, in *Organoids: Stem Cells, Structure, and Function* (Ed: K. Turksen), Springer, New York **2019**, p. 291.
[18] L. Gao, T. J. McCarthy, *Langmuir* **2007**, *23*, 10445.
[19] R. K. Vadivelu, H. Kamble, A. Munaz, N.-T. Nguyen, *Sci. Rep.* **2017**, *7*, 12388.
[20] R. Vadivelu, N. Kashaninejad, K. R. Sreejith, R. Bhattacharjee, I. Cock, N.-T. Nguyen, *ACS Appl. Mater. Interfaces* **2018**, *10*, 43439.
[21] V. Das, T. Fürst, S. Gurská, P. Džubák, M. Hajdúch, *J. Visualized Exp.* **2017**, *121*, e55403.
[22] M. K. Khaw, C. H. Ooi, F. Mohd-Yasin, R. Vadivelu, J. St John, N.-T. Nguyen, *Lab Chip* **2016**, *16*, 2211.
[23] A. Pluen, P. A. Netti, R. K. Jain, D. A. Berk, *Biophys. J.* **1999**, *77*, 542.
[24] M. Nikmaneshi, B. Firoozabadi, M. Saidi, *J. Biomech.* **2018**, *67*, 37.
[25] A. Tosun, H. Erbil, *Appl. Surf. Sci.* **2009**, *256*, 1278.
[26] J. Narayanan, J.-Y. Xiong, X.-Y. Liu, *J. Phys.: Conf. Ser.* **2006**, *28*, 83.
[27] V. Wiegmann, C. B. Martinez, F. Baganz, *Biotechnol. Lett.* **2018**, *40*, 1029.
[28] A. Ebrahimi, M. A. Alam, *Proc. Natl. Acad. Sci. USA* **2016**, *113*, 7059.
[29] A. Walzl, N. Kramer, G. Mazza, M. Rosner, D. Falkenhagen, M. Hengstschlaeger, D. Schwanzer-Pfeiffer, H. Dolznig, *Int. J. Appl. Sci. Biotechnol.* **2012**, *2*, 17.